From ferromagnetic to antiferromagnetic interactions in *n*-type $Zn_{1-x}Mn_xO$: An electron paramagnetic resonance study

A. Ben Mahmoud
Institut des NanoSciences de Paris, Universités Paris 6 et 7, UMR 7588 au CNRS (France), 140 rue de Lourmel, 75015 Paris, France and Laboratoire Physique des Matériaux et des Nanomatériaux appliquée à l'Environnement, Faculté des Sciences, Cité Erriadh, 6079 Gabès, Tunisia

H. J. von Bardeleben and J. L. Cantin
Institut des NanoSciences de Paris, Universités Paris 6 et 7, UMR 7588 au CNRS (France), 140 rue de Lourmel, 75015 Paris, France

A. Mauger
Département Mathématiques, Informatique, Physique, Planète et Univers, CNRS, Campus Boucicaut, 140 rue de Lourmel, 75015 Paris, France

E. Chikoidze and Y. Dumont
Laboratoire de Physique des Solides et de Cristallogenèse, CNRS-Université de Versailles St-Quentin en Yvelines, 1 place Aristide Briand, 92195 Meudon, France

(Received 24 June 2006; published 12 September 2006)

Contradictory results concerning the formation of a ferromagnetic state in Mn doped ZnO layers have been reported in the last years. We present the results of an electron paramagnetic resonance study on homogeneous single phase *n*-type conductive $Zn_{1-x}Mn_xO$ ($x<0.07$) thin films. Based on the observation of the existence of a narrow Mn composition range, $x<0.05$, where a ferromagnetic interaction is dominant, whereas for larger x nearest neighbor antiferromagnetic interactions dominate, we propose a magnetic polaron model for the ferromagnetic Mn-Mn interaction in *n*-type films.

DOI: 10.1103/PhysRevB.74.115203 PACS number(s): 75.50.Pp, 71.55.Gs, 75.30.Hx

I. INTRODUCTION

The magnetic properties of 3*d* transition metal (TM) doped ZnO thin films have been the object of intense research in the last years due to the potential formation of a ferromagnetic phase with a Curie temperature above room temperature.[1–3] The origin of this ferromagnetism is however, not yet clear. The TM dopants substitute for the Zn cation and may be in addition electrically active. As concerns Mn doping, Mn_{Zn} is twofold charged (2+) with a ^6S ground state and does not introduce any free carriers. In this case, *ab initio* calculations within the local spin density approximation (LSDA) have shown that the superexchange interactions between two nearest neighbor substitutional magnetic ions are antiferromagnetic.[4] The same result has been obtained for ZnO:Co. In this latter case earlier LSDA calculations predicted ferromagnetic interactions, but it has been argued in Ref. 4 that this result is an artifact when Coulomb correlations are neglected. Therefore, we know now that any ferromagnetism in $Zn_{1-x}Mn_xO$ cannot be attributed to an Mn-Mn interaction only. Apart from intrinsic ferromagnetism[5–7] additional mechanisms have been proposed in the literature to explain the observation of room temperature ferromagnetism: they include the formation of secondary magnetic phases,[8,9] interactions with cation vacancies or other defects,[10–14] disorder,[15] in brief anything which can introduce free carriers and make the material *p* or *n* type. The two kinds of doping, however, are not equivalent due to the different strengths of the interactions. In *p* type material the *p-d* hybridization gives rise to a strong ferromagnetic Zener double-exchange interaction. On the other hand in *n*-type material the electrons in the conduction band move essentially in the Zn 4*s* orbital and all the manganese ions stay in the divalent state with the consequence that there is no double exchange interaction. As the partial density of Mn *d* states near the bottom of the conduction band is negligible and the *s-d* interaction is weak, ferromagnetism is not expected in *n*-type $Zn_{1-x}Mn_xO$ which is the normal conduction in nonintentionally co-doped material.[2]

Nevertheless, ferromagnetism has been observed in various *n*-type $Zn_{1-x}Mn_xO$ layers.[5–14] Other experimental studies of $Zn_{1-x}Mn_xO$ reported the opposite, namely the existence of antiferromagnetic interactions only[16–20] and it became evident that the sample preparation played a crucial role. Mn clustering and second phase inclusions might be favored by out of equilibrium growth techniques such as pulsed laser deposition (PLD), sputtering or solid state reaction. Equilibrium deposition techniques such as molecular beam epitaxy (MBE) or metal organic chemical vapor deposition (MOCVD) seem more suited to obtain a homogeneous dopant distribution assumed in modeling. In general, the layers are *n*-type conductive due to the presence of uncontrolled dopants such as H, Zn interstitials, oxygen vacancies, or extrinsic shallow donors (Al). The role of such donors in the magnetism of the ZnO:TM films has not yet been sufficiently considered.

The first aim of this paper is to improve the present understanding of the origin of ferromagnetism in $Zn_{1-x}Mn_xO$ layers. For this purpose, we have undertaken an electron paramagnetic resonance (EPR) study of MOCVD-grown thin

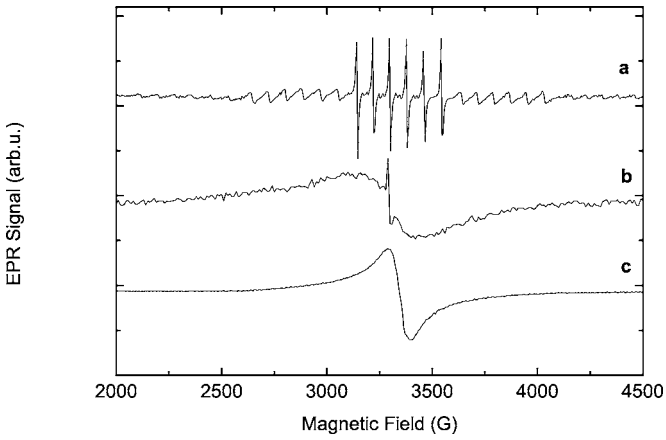

FIG. 1. Experimental *X*-band EPR spectra of $Zn_{1-x}Mn_xO$ at $T=300$ K; (a) $x=0.006$, (b) $x=0.026$, (c) $x=0.07$; the sharp line in (b) is substrate related.

$Zn_{1-x}Mn_xO$ layers. We have extended a previous EPR study[20] on $Zn_{0.84}Mn_{0.16}O$ to lower Mn doping concentrations $0.006<x<0.16$. Our results show that there is a drastic change in the magnetic properties at $x\sim0.05$ with dominant ferromagnetic interactions at smaller x and antiferromagnetic ones for all larger x. The use of the EPR technique offers some interesting advantages over the generally used superconducting quantum interference device (SQUID) magnetization measurements: it has a higher sensitivity which is required for studies of thin films of lightly doped diluted magnetic semiconductors (DMS) and its resonant character allows one to easily eliminate substrate contributions and effects of second phase inclusions.

II. EXPERIMENTAL DETAILS

The study has been performed on epitaxial layers grown by MOCVD on (0001) Al_2O_3 substrates. The precursors were diethyl-zinc (DEZ) and tertiary-butanol (tBu), as zinc and oxygen sources, respectively, and liquid $(CO)_3CH_3C_5H_4Mn$ as the manganese precursor. Hydrogen was used as a vector gas. The substrate temperature was 450 °C; the typical thickness of the films was 1 μm. Manganese atomic fraction x of investigated $Zn_{1-x}Mn_xO$ samples varies from $x=0.006$ to $x=0.16$. The Mn concentrations controlled by the gas flow ratios were verified by x-ray emission (EDX) measurements, and also by the measurement of the lattice parameter which is linear in x and follows the Vegard's law.[21] The absence of extrinsic phases was checked by x-ray diffraction. No additional phase has been detected. The ZnMnO films are highly textured with a *c*-axis orientation normal to the sapphire plane. The as-prepared films were *n*-type conductive with a room temperature carrier concentration of 10^{18} cm^{-3} probably related to hydrogen incorporation and other defects.[21] The EPR measurements were performed with a standard *X*-band spectrometer in the temperature range 4–300 K.

III. EXPERIMENTAL RESULTS

In Fig. 1 we show the room temperature EPR spectra

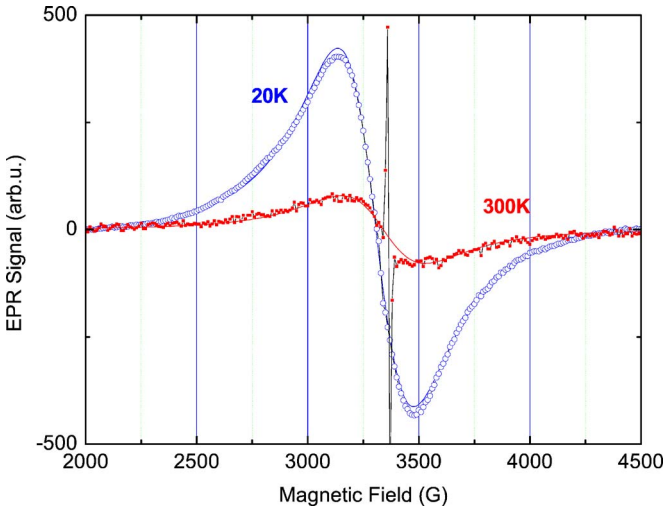

FIG. 2. (Color online) Experimental EPR spectra of $Zn_{0.974}Mn_{0.026}O$ at 300 K and 20 K as well as line shape simulations with a Lorenztian line shape.

observed for three different Mn concentrations $x=0.006$, 0.026, 0.07 with the magnetic field oriented normal to the layer plane. At the lowest concentration we observe the anisotropic 30 line spectrum of isolated substitutional Mn_{Zn}^{2+} ions in C_{3V} symmetry.[22] This spectrum, corresponding to a paramagnetic state, has been analyzed previously[23] and will not be discussed here. At the higher Mn concentration of $x=0.026$ the multiline spectrum of the isolated Mn ion is no longer observable and is replaced by a 400 G broad single line of Lorentzian line shape. At a still higher Mn concentration of $x=0.07$ we observe again a single line spectrum with a line width of 110 G which decreases further to ~90 G for Mn concentrations $x\geqslant0.12$.

The high and low temperature EPR spectra of the two concentrations discussed here are compared in Figs. 2 and 3. For the $x=0.026$ sample the line shape is Lorentzian and the linewidth at 300 K and 20 K are 400 G and 350 G, respectively. For the higher Mn concentration $x=0.07$ the exchange

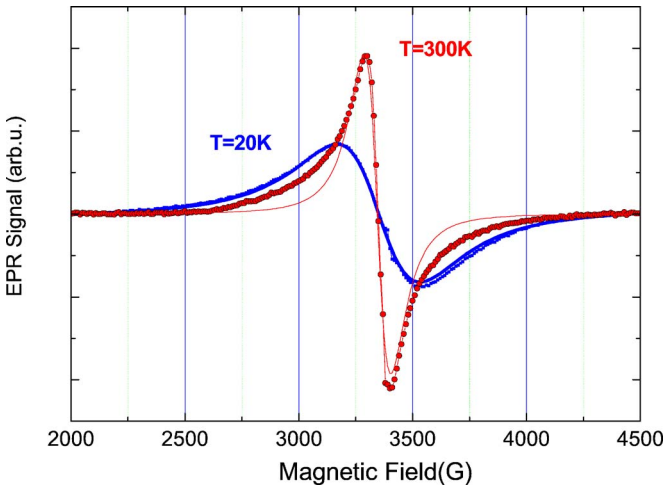

FIG. 3. (Color online) Experimental EPR spectra of $Zn_{0.93}Mn_{0.07}O$ at 300 K and 20 K as well as line shape simulations with a Lorenztian line shape.

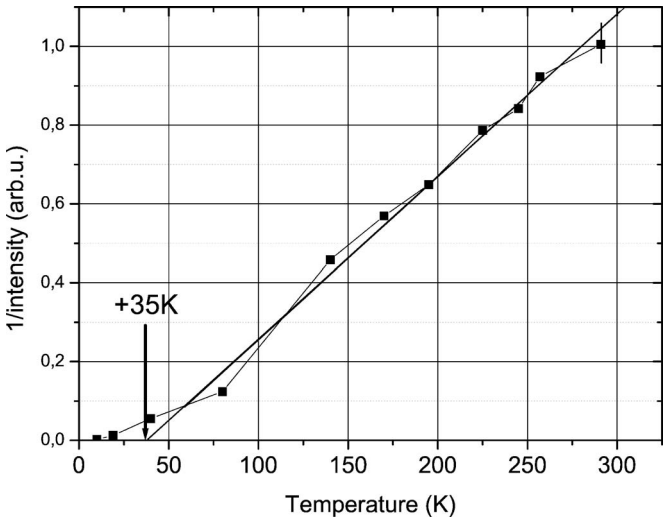

FIG. 4. Variation of the inverse of the EPR intensity vs temperature for $x=0.026$. A typical error bar is indicated for the RT value. The straight line is the fit by the Curie-Weiss law.

narrowing reduces the high temperature linewidth to 110 G whereas the low temperature linewidth is now 340 G.

The magnetic properties of the layers can be analyzed from the variation of the intensity of the EPR spectra with temperature. The intensity $I(T)$ obtained by a double integration of the experimental EPR spectrum is directly proportional to the magnetic susceptibility χ. In the high temperature limit, it is commonly accepted that the variation of the EPR intensity $I(T)$ can be described by (Ref. 24):

$$I = \frac{C(x)}{T - \theta(x)} = \frac{C_0 x}{T - \theta_0 x}, \tag{1}$$

where C is the Curie constant, θ the Curie-Weiss temperature, and C_0 and θ_0 the corresponding doping concentration independent values. The sign of the Curie-Weiss temperature

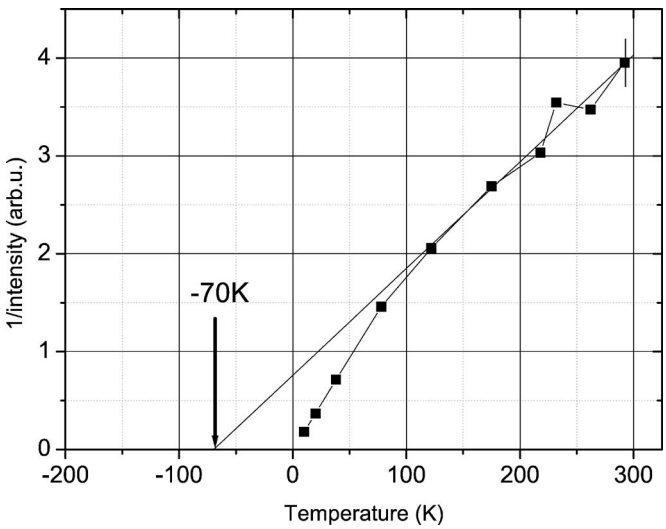

FIG. 5. Variation of the inverse of the EPR intensity vs temperature for $x=0.07$. A typical error bar is indicated for the RT value. The straight line is the fit by the Curie-Weiss law.

will directly indicate whether the magnetic interactions are ferromagnetic ($\theta>0$) or antiferromagnetic ($\theta<0$). In Figs. 4 and 5 we show the results obtained for the $Zn_{1-x}Mn_xO$ layers with $x=0.026$ and $x=0.07$. We observe a linear Curie-Weiss behavior at high temperatures for both concentrations. The respective Curie-Weiss temperatures are obtained from the linear extrapolation of the high temperature part of the curves. We obtain a positive Curie-Weiss temperature $\theta=+35$ K for the $x=0.026$ film and a negative Curie-Weiss temperature $\theta=-70$ K for the $x=0.07$ film. For higher Mn concentrations, θ remains negative and $|\theta|$ increases monotonously with x. Thus surprisingly, in the low doped layer the Mn ions are ferromagnetically coupled.

The Curie-Weiss analysis for diluted magnetic semiconductors is suitable because the magnetic contribution of the Mn ions is dominated by isolated ions or ions on nearest neighbor (NN) sites. The topology of the distribution changes with the Mn composition. The Mn ions are distributed in clusters of increasing size, up to the percolation threshold of $x=0.16$. For concentrations higher than $x=0.16$ the Mn ions can be treated as one cluster of infinite size which is expected to generate deviations from a linear variation with x [Eq. (1)]. It is clear that the second equality in Eq. (1) is valid for the low concentrations studied here. We can deduce the effective exchange integral J_1 for nearest neighbor pairs from the measured Curie-Weiss temperatures according to:

$$\frac{J_1}{k_B} = -\frac{3}{2}\frac{\theta_0}{S(S+1)z_1}. \tag{2}$$

z_1 is the number of NN sites (equivalent or not) in the wurtzite lattice, i.e., $z_1=12$.

For the antiferromagnetic $x=0.07$ sample we obtain from the Curie-Weiss temperature of -70 K an effective exchange integral of $J_1/k_B=-21.8$ K. From magnetization step measurements experimental values of $J_{1,\parallel}/k_B=-23$ K, $J_{1\perp}/k_B=-15$ K have been reported,[25] leading to an average value of $J_1/k_B=-21$ K. Our result is thus in quantitative agreement with these experiments.

The variation of the linewidth ΔB of the EPR spectrum with temperature for the $x=0.07$ (and higher concentrations) film is also characteristic of a semimagnetic semiconductor with antiferromagnetic interactions. In this case the variation of ΔB with T is often described by an empirical expression (Refs. 24 and 26):

$$\Delta B(T) = (\Delta B)_\infty (T\chi_0)^{-1}\Gamma(T,x) \approx (\Delta B)_\infty \cdot \left(1 + \frac{\vartheta}{T}\right), \tag{3}$$

where ΔB_∞ is the infinite temperature linewidth, χ_0 the static susceptibility, and x the Mn atomic fraction. Generally it can be assumed that $\Gamma(T,x)$ is temperature independent above the spin glass transition, so that Eq. (4) predicts a $(1+\theta/T)$ temperature variation. For the $x=0.07$ sample we indeed observe qualitatively such a high temperature variation.[26,27] In the spin glass state $T<50$ K the linewidth is nearly constant.

For the $x=0.026$ sample the origin of the ferromagnetic interaction must be different. The analysis of the Curie temperature within the model of Eq. (2) is not applicable as the

Mn interactions stay AF even for more distant pairs.[4] The temperature variation of the linewidth with a nearly constant value between 4 and 300 K is equally different from the AF case.

IV. DISCUSSION

As the EPR spectra show the absence of any charge state other than Mn^{2+} we know that the double exchange interaction is inefficient. The origin of the ferromagnetism in our samples is thus of a quite different nature than in the case of Zn-Mn-O systems where the coexistence of different ionization states of Mn has been detected.[8] In magnetic semiconductors it is well known that an electron bound to a donor can increase its binding energy by polarizing the localized spins in its neighborhood to form a magnetic polaron. This increase in binding energy turns a simple hydrogenic donor into a magnetic polaron with a deep donor state. It carries a macroscopic spin associated to the cloud of the localized spins that are spin-polarized by the *s-d* exchange interaction:

$$E_{ex} = -N_0\alpha\frac{a^3}{4}\sum_i |\Psi(R_i)|^2 \vec{S}_i \,.\, \vec{s} \qquad (4)$$

with $N_0\alpha$ the exchange integral, $a^3/4$ is the volume of the unit cell of the lattice, and Ψ the wave function of the electron bound to the donor. The summation runs over all lattice sites R_i occupied by a Mn^{2+} ion in the neighborhood of the donor site. S and s refer to the Mn^{2+} spin and the donor electron spin, respectively.

The macroscopic magnetic moment associated with such a magnetic polaron can be large even in an antiferromagnetic environment[28] provided we are dealing with a true magnetic semiconductor with one localized spin per unit cell. In the present case, we are dealing with a dilute semimagnetic semiconductor with $x<0.05$. As the gain in binding energy associated to the *s-d* exchange interaction is proportional to x, it becomes negligible for $x<0.05$. To make it clear, the loss in kinetic energy in any shrinking in the electron orbital will overcome the gain in magnetic energy so that the donor level remains shallow. This is in essence why there are actually shallow donor states in $Zn_{1-x}Mn_xO$ which are at the origin of the 10^{18} cm^{-3} free carriers in the samples we have studied. Moreover, since the donor level is shallow, such an amount of donor electrons should exceed the critical concentration for the insulator-metal transition, so that the electrons on the donors are delocalized, not only at room temperature, but also at low temperature. The only effect of the shallow donors in this configuration is to provide free carriers in the conduction band. In this case the *s-d* exchange interaction gives rise to the indirect Ruderman-Kittel-Kasuya-Yosida (RKKY) interaction. Indeed, this interaction may generate a ferromagnetic ordering between Mn^{2+} ions, but only for free carrier concentrations the order of 10^{20} cm^{-3} (Ref. 29). In the present case, the low concentration of carriers ($n\sim10^{18}$ cm^{-3}) is not sufficient to induce a ferromagnetic coupling between loose Mn^{2+} ions.

To account for the ferromagnetic interactions in our low doped materials, we are then led to assume the existence of deeper donor levels, in addition to the shallow donor levels which provide us with the conduction electrons at room temperature. The importance of deep donors to generate high temperature ferromagnetism has been reported in ZnO:Co where the interstitial H donor is a good candidate.[30] In this case, an important dimerization of Co was assumed, each dimer capturing a hydrogen atom. In $Zn_{1-x}Mn_xO$, we have no evidence of any tendency of dimerization of Mn. On the contrary, the magnetic properties of our films with $x>0.05$ scale with those of $Cd_{1-x}Mn_xTe$ where the Mn distribution is known to be random; the concentration of unpaired Mn^{2+} ions when it has been measured corroborates equally a random distribution.[18] However, a moderately deep donor related to hydrogen already exists in many nonintentionally doped ZnO single crystals.[31] As hydrogen is the carrier gas during film deposition, the high solubility of hydrogen in ZnO makes very likely the presence of hydrogen related donors in our $Zn_{1-x}Mn_xO$ layers; it will give rise to an exchange interaction of the same form as in Eq. (4). In that case, $N_0\alpha$ is allowed to be different from the value it takes with free electrons in the conduction band, namely 0.19 eV (Ref. 32), but it should keep the same order of magnitude. Then Eq. (4) allows us to evaluate the donor properties required to induce a ferromagnetic exchange interaction between the Mn ions. It should be noted that the NN antiferromagnetic interaction between Mn-Mn close pairs is so strong that in a first approximation the ferromagnetic interaction given by Eq. (4) will have no effect on them. This has been accounted for by limiting the summation in Eq. (4) only to the sites occupied by unpaired Mn^{2+} ions. As the donor is rather deep, the exchange and the central cell corrections are important, so that the wave function of the electron bound to the donor will be far from a Slater-type orbital. Since it is basically unknown it is sufficient to mimic the localization effects by assuming a wave function uniformly distributed within a radius R. To estimate the order of magnitude expected for the donor-mediated ferromagnetic coupling between the isolated spins, let us then consider a donor wave function uniformly distributed over 70 unit cells: $(a^3/4)|\Psi(R_i)|^2=1.410^{-2}$ inside the orbital. Then for $x=0.03$ and assuming a random distribution there are on average two isolated Mn spins inside the donor orbital assuming which will be coupled by a ferromagnetic interaction. For $N_0\alpha=0.19$ eV, the exchange energy per isolated spin inside the donor orbital $(a^3/4)|\Psi(Ri)|^2Ss\sim30$ K, which is roughly the value of θ observed for the $x=0.026$ sample. Therefore, such donors are able to generate the ferromagnetic interaction between unpaired spins observed in our experimental result.

Note that this ferromagnetic coupling is not able to generate ferromagnetic ordering at room temperature, and indeed, the material in the experiments is paramagnetic at room temperature. On another hand, at low temperature, it will contribute to spin polarize the loose spins in a ferromagnetic arrangement, hence the increase in the spin polarization evidenced by the upward curvature of the $I(T)^{-1}$ curve observed below 30 K in Fig. 4. This effect can only be observed at low Mn concentrations, because the Mn spins must be predominantly isolated, i.e., without any NN neighbor. This is the basic reason why the ferromagnetic interaction is

only observed at low Mn concentrations of $x<0.05$. Note this upward curvature below 30 K does not mean that the material undergoes a transition to a ferromagnetic ordering at this temperature. Actually, such an ordering is not expected. Instead, the system should undergo a spin glass freezing at low temperature, similar to those observed in magnetic semiconductors with ferromagnetic interactions not negligible with respect to the AF ones.[33]

CONCLUSIONS

The magnetic interactions in intrinsic $Zn_{1-x}Mn_xO$ are antiferromagnetic. Our results show that ferromagnetic interactions are not an intrinsic property as envisioned in earlier works.[5–7] They are neither due to secondary magnetic phases[8,9] nor due to the effect of disorder effects.[15] They can be quantitatively simulated to the coexistence of shallow and moderately deep donors that can induce an effective ferromagnetic coupling between unpaired Mn ions at small x. We also note that, in our approach, the amount of these donors do not have to be in such a large quantity that they generate impurity bands.[10] The experimental data are fully consistent with this analysis. Note, however, that such donors can by no means explain a long-range ferromagnetic ordering at room temperature reported in the literature in some heavily Mn doped $Zn_{1-x}Mn_xO$ samples, especially as there is experimental evidence that the Mn distribution in $Zn_{1-x}Mn_xO$ is random. High Curie temperatures in this case require different mechanisms, such as double exchange interactions in p-type materials. In n-type materials, high Curie temperature would require much larger free carrier concentrations. Even though it should be noted that the range of the RKKY interaction is limited to the mean free path of the free carriers, and the large decrease in the mobility with x will make this interaction actually short range. A coupling between magnetic polarons in n-type samples would then require a huge concentration ($\sim 10^{20}$ cm^{-3}) of the moderately deep donors envisioned in this work. In this case the material would become ferromagnetic yet the Curie temperature is expected to be low, i.e., the order of the Curie-Weiss temperature θ.

*Corresponding author: jurgen.vonBardeleben@insp.jussieu.fr

[1] K. Sato and H. Katayama-Yoshida, Jpn. J. Appl. Phys., Part 1 **39**, 555 (2000); **40**, L334 (2001).
[2] T. Dietl, H. Ohno, F. Matsukura, J. Cibert, and D. Ferrand, Science **287**, 1015 (2000).
[3] R. Janisch, P. Gopal, and N. A. Spaldin, J. Phys.: Condens. Matter **17**, R657 (2005).
[4] T. Chanier, M. Sargolzaei, I. Opahle, R. Hayn, and K. Koepernik, Phys. Rev. B **73**, 134418 (2006).
[5] P. Sharma, A. Gupta, K. V. Rao, F. J. Owens, R. Sharma, R. Ahulja, J. M. O. Guillen, B. Johansson, and G. A. Gehring, Nat. Mater. **2**, 673 (2003).
[6] P. Sharma, A. Gupta, F. J. Owens, A. Inoue, and K. V. Rao, J. Magn. Magn. Mater. **282**, 115 (2005).
[7] A. K. Pradham, D. Hunter, K. Zhang, J. B. Dadson, S. Mohanty, T. M. Williams, K. Lord, R. R. Rakhimov, U. N. Roy, Y. Cui, A. Burger, J. Zhang, and D. J. Sellmyer, Appl. Surf. Sci. **252**, 1628 (2005).
[8] M. A. Garcia, M. L. Ruiz-Gonzalez, A. Quesada, J. L. Costa-Kramer, J. F. Fernandez, S. J. Khatib, A. Wennberg, A. C. Caballero, M. S. Martin-Gonzalez, M. Villegas, F. Briones, J. M. Gonzales-Calbet, and A. Hernando, Phys. Rev. Lett. **94**, 217206 (2005).
[9] D. Kundaliya, S. G. Ogale, S. E. Lofland, S. Dhar, C. J. Metting, S. R. Shinde, Z. Ma, B. Varughese, K. V. Ramanujachary, L. Salamanca-Riba, and T. Venkatesan, Nat. Mater. **3**, 709 (2004).
[10] M. Venkatesan, C. B. Fitzgerald, J. G. Lunney, and J. M. D. Coey, Phys. Rev. Lett. **93**, 177206 (2004).
[11] J. M. D. Coey, M. Venkatesan, and C. B. Fitzgerald, Nat. Mater. **4**, 173 (2005).
[12] P. V. Radovanovic and D. R. Gamelin, Phys. Rev. Lett. **91**, 157202 (2003).
[13] N. A. Theodoropoulou, A. F. Hebard, D. P. Norton, J. D. Budai, L. A. Boatner, J. S. Lee, Z. G. Kim, Y. D. Park, M. E. Overberg, S. J. Pearton, and R. G. Wilson, Solid-State Electron. **47**, 2231 (2003).
[14] N. Theodoropoulou, V. Misra, J. Philip, P. LeClair, G. P. Berera, J. S. Moodera, B. Satpati, and T. Som, J. Magn. Magn. Mater. **300**, 407 (2005).
[15] M. Berciu and R. N. Bhatt, Phys. Rev. B **69**, 045202 (2004).
[16] T. T. Fukurama, Z. Jin, M. Kawasaki, T. Shono, T. Hasegawa, S. Koshihara, and H. Koinuma, Appl. Phys. Lett. **78**, 958 (2001).
[17] S. Kolesnik, B. Dabrowski, and J. Mais, J. Appl. Phys. **95**, 2582 (2004).
[18] G. Lawes, A. S. Risbud, A. P. Ramirez, and R. Seshadri, Phys. Rev. B **71**, 045201 (2005).
[19] M. H. Kane, K. Shalini, C. J. Summers, R. Varatharan, J. Nause, C. R. Vestal, Z. J. Zhang, and I. T. Ferguson, J. Appl. Phys. **97**, 023906 (2005).
[20] E. Chikoidze, H. J. von Bardeleben, Y. Dumont, J. L. Cantin, and P. Galtier, J. Appl. Phys. **97**, 10D316 (2005).
[21] E. Chikoidze, Y. Dumont, F. Jomard, D. Ballutaud, P. Galtier, O. Gorochov, and D. Ferrand, J. Appl. Phys. **97**, 10D327 (2005).
[22] A. Hausmann and H. Huppertz, J. Phys. Chem. Solids **29**, 1369 (1968).
[23] M. Diaconu, H. Schmidt, A. Poppl, R. Böttcher, J. Hoentsch, A. Klunker, D. Spemann, H. Hochmuth, M. Lorenz, and M. Grundmann, Phys. Rev. B **72**, 085214 (2005).
[24] J. K. Furdyna and N. Samarth, J. Appl. Phys. **61**, 3526 (1987).
[25] X. Gratens, V. Bindilatti, N. F. Oliveira, Y. Shapira, S. Foner, Z. Golacki, and T. E. Haas, Phys. Rev. B **69**, 125209 (2004).
[26] N. Samarth and J. K. Furdyna, Phys. Rev. B **37**, 9227 (1988).
[27] J. W. Battles, J. Appl. Phys. **42**, 1286 (1971).
[28] A. Mauger and D. L. Mills, Phys. Rev. B **31**, 8024 (1985).
[29] A. Mauger and M. Escorne, Phys. Rev. B **35**, 1902 (1987).
[30] C. H. Park and D. J. Chadi, Phys. Rev. Lett. **94**, 127204 (2005).
[31] D. M. Hofmann, A. Hofstaetter, F. Leiter, H. Zhou, F. Henecker, B. K. Meyer, S. B. Orlinskii, J. Schmidt, and P. G. Baranov, Phys. Rev. Lett. **88**, 045504 (2002).
[32] T. Dietl, in *Handbook on Semiconductors*, edited by T. S. Moss (North Holland, Amsterdam, 1994), Vol. 3b, p. 1251.
[33] N. Bontemps and R. Orbach, Phys. Rev. B **37**, 4708 (1988), and references therein.